

IN-76-TM  
65422  
p. 24

## GROWTH OF BINARY ORGANIC NLO CRYSTALS: m.NA-p.NA and m.NA-CNA System

N. B. Singh, T. Henningsen, R. H. Hopkins, and R. Mazelsky  
Westinghouse Science & Technology Center  
Pittsburgh, PA 15235-5098

F. K. Hopkins  
Materials Directorate, Wright Laboratory  
WPAFB, OH 45433

D. O. Frazier  
NASA George Marshall Space Flight Center  
Huntsville, AL 35812

O. P. Singh  
Chemistry Department, K.N. Government Post-Graduate College  
Gyanpur, UP, India

ORIGINAL PAGE IS  
OF POOR QUALITY

### ABSTRACT

Experiments were carried out to grow 3-Nitroaniline (m.NA) crystals doped with 4-Nitroaniline (p.NA) and 2-chloro 4-Nitroaniline (CNA). The measured undercooling for m.NA, p.NA, and CNA were 0.21 tm K, 0.23 tm K and 0.35 tm K respectively, where tm represents the melting temperature of the pure component. Because of the crystals' large heat of fusion and large undercooling, it was not possible to grow good quality crystals with low thermal gradients. In the conventional two-zone Bridgman furnace we had to raise the temperature of the hot zone above the

(NASA-TM-111073) GROWTH OF BINARY  
ORGANIC NLO CRYSTALS: m.NA-p.NA AND  
m.NA-CNA SYSTEM (NASA. Marshall  
Space Flight Center) 24 p

N96-16014

Unclass

ORIGINAL PAGE IS  
OF POOR QUALITY

decomposition temperature of CNA, p.NA, and m.NA to achieve the desired thermal gradient. To avoid decomposition, we used an unconventional Bridgman furnace. Two immiscible liquids, silicone oil and ethylene glycol, were used to build a special two-zone Bridgman furnace. A temperature gradient of 18 K/cm temperature gradient was achieved without exceeding the decomposition temperature of the crystal. The binary crystals, m.NA-p.NA and m.NA-CNA, were grown in centimeter size in this furnace. X-ray and optical characterization showed good optical quality.

# 1. BACKGROUND

Crystal growth techniques for inorganic optical materials from the melt were developed in a relatively short span of time because a huge body of relevant literature was available on the solidification of metals and alloys. The situation was very different for the organic optical materials. Most of the crystal growth studies for organic materials were based upon the model [1] to simulate the solidification behavior of high temperature materials. Most of the metals and alloys freeze with a nonfaceted interface, which involves a low heat of fusion during phase transformation. On the other hand, organic materials which typically exhibit optical nonlinearities have high values of  $\Delta_f h/R$  and grow with facets.  $\Delta_f h$  is the heat of fusion and R is the gas constant. Growth of this class of materials is generally anisotropic and spikey, and materials generally need a high degree of undercooling to initiate nucleation and to grow. Because these materials require large undercooling, they often contain a large density of imperfections. For this situation, a high thermal gradient is required to grow good quality crystals. We have extensively studied [2,3] the purification, solidification behavior and crystal characteristics of pure organic crystals. We also observed [4] that binary organics show higher optical nonlinearities compared to parent components. But growth of binary organics require even higher thermal gradients to achieve good quality. The present study reports a novel technique to achieve higher gradients by using two immiscible liquids. Crystals of the

m.NA-p.NA and m.NA-CNA systems were grown, and their optical quality was evaluated.

## **2. EXPERIMENTAL METHODS**

### **2.1 PURIFICATION OF SOURCE MATERIALS**

The starting materials, m.NA, p.NA and CNA, were supplied with 99.0% purity. m.NA and p.NA were then further purified by a combination of repeated distillations followed by directional freezing in vacuum. The first and last part of the frozen material was discarded since impurities tend to segregate to these regions. CNA was purified by an evaporation method. Vacuum-sealed as-supplied material was placed in a two zone furnace, with the bottom zone of the furnace at a higher temperature than the top zone. The temperature of the bottom zone was raised close to the melting temperature of CNA to achieve a good rate of evaporation.

### **2.2 HEAT OF FUSION MEASUREMENT**

The heat of fusion of purified material was measured by Perkin Elmer DSC, with computer-aided data acquisition analysis. Samples were prepared in hermetically sealed aluminum pans. All runs were carried out in the range of 2 mcal/sec, with a chart speed of 5 mm/min, and with a chart range of 10 mV. The heating range was 1.5 K/min.

### **2.3 UNDERCOOLING MEASUREMENT**

The undercooling measurements were carried out in a manner described in reference 5.

## **2.4 THE CRYSTAL GROWTH FURNACE AND GROWTH OF CRYSTALS**

We designed a two-zone Bridgman furnace employing silicone oil and ethylene glycol as the heat transfer media. These liquids do not mix and maintain sharp phase boundaries, with the silicon oil in the hot zone and the ethylene glycol in the cold zone. The temperature of the hot zone was controlled to within 0.5K. The desired translation rate of the furnace was maintained with a motor-driven gear.

### **Optical Characterization**

The boules were grown in the form of a cylinder, 11 mm in diameter and 30 mm long. Crystals were cut with a string saw, and crystals were fabricated with their polished surfaces parallel to the cleavage plane. The bulk transparency was examined to identify the gross defects such as precipitates, bands and cracks in the crystals. The transmittance of both crystals was measured in the range of 0.25 to 3.0 micrometer using a Varian Model 2300 photospectrometer. X-ray Laue patterns were taken to identify the growth orientations and evaluate the crystallinity of the crystals.

### 3. RESULTS AND DISCUSSION

The purification techniques for m.NA, p.NA and CNA are limited due to contamination of these compounds with air and partial decomposition of these compounds above their melting temperatures. The distilled material was directionally solidified in a sealed evacuated quartz tube to avoid contamination. Yet, the partial decomposition at a temperature above melting ( $150^{\circ}\text{C}$ ) created pyrolysis. Black particles and side products were embodied in the directionally frozen material as shown in Figure 1. However, it was found that the pyrolysis could be suppressed by working at lower temperatures.

The measured values of heat of fusion for m.NA, CNA and p.NA are listed in Table 1. This shows that  $\Delta_{\text{ch}}/R$  is larger than 2, and these compounds belong to faceted classes. Their solidification behavior will differ from metals and alloys because of the high heat transfer during the solidification. The measured undercooling for m.NA, p.NA, and CNA were  $0.21\text{ }t_{\text{m}}\text{ K}$ ,  $0.23\text{ }t_{\text{m}}\text{ K}$ , and  $0.35\text{ }t_{\text{m}}\text{ K}$  respectively, where  $t_{\text{m}}$  represents the melting temperature of the pure component. This observation was typical of materials with a large heat of fusion which have a tendency to undercool significantly below the melting point. Because of the large heat of fusion and the large undercooling, it was not possible to grow good quality crystals at a low thermal gradients. In the conventional two-zone Bridgman furnace, we had to raise the temperature of the hot zone above the decomposition temperature of CNA, p.NA, and m.NA to achieve the desired thermal

gradient. To avoid the decomposition, we used an unconventional Bridgman furnace.

Two immiscible liquids, silicone oil and ethylene glycol, were used to build a special two-zone Bridgman furnace. Figure 2 shows the temperature distributions of the same furnace without and with the silicone oil/ethylene glycol as the heat transfer medium at the identical controller setting. A temperature gradient of 18 K/cm was achieved without exceeding the decomposition temperature of the crystal.

The phase-diagram for m.NA-p.NA for the low concentration region of p.NA is shown in Figure 3. The dotted line shows the ideal curve predicted [4] from the physical parameters. The phase-diagram is in good agreement with that predicted by Ozawa and Matsuoka [3] for this system. The solid-liquid equilibrium data on this system along with m.NA-CNA system [4] showed that p.NA or CNA will segregate in the liquid during the directional solidification. Because of this reason, we used a low doping concentration (less than 5 wt %) of CNA and p.NA in this study. Due to the large value of  $\Delta_f h/R$ , crystals froze with a high heat transfer, and morphology was always faceted. To facilitate the nucleation, we used a 3-centimeter long capillary attached to the main body of the growth tube. In the case of the m.NA-CNA system, we also carried out several growth runs with a preoriented seed. The growth speed was 0.7 to 1.0 cm/day.

When we used the capillary to grow m.NA-p.NA and m.NA-CNA crystals, the crystals grew in the c-direction and the cleavage plane was the b-plane which is identical to pure m.NA. The X-ray Laue patterns were much better on the cleavage plane and as grown surfaces. Surfaces etched with acetone-water or alcohol-water mixtures did not



produce good quality surfaces. The pure m.NA crystal has a stronger tendency to cleave and has more river pattern structure than doped m.NA crystals. The transparency of m.NA-p.NA and m.NA-CNA crystals is shown in Figures 4 and 5 with and without a wire mesh. Both crystals were free from gross defects such as microprecipitates, microcracks and voids. We did not observe any optical distortion in the mesh image indicating good crystal quality. The transmission curves for the m.NA-CNA and m.NA-p.NA crystals are shown in Figure 6. The transmission curve for the m.NA-CNA crystal showed only characteristics bands. We did not observe any absorption bands due to residual impurities. The m.NA-p.NA crystal showed continuous improvement in the transmission between 0.5 to 0.85 micrometer wavelength region (Figure 6). Also, the m.NA-p.NA crystal showed several absorption bands in this region due to residual impurities. The comparison of both transmission curves suggests that with the improved purification procedures, it should be possible to produce m.NA-p.NA crystals free of absorption bands in the visible and near-infrared regions.

A second harmonic conversion experiment was carried out for the CNA-m.NA crystals. A Q-switched YAG laser operating at 1.06 micrometer with a pulse length of 10 ns was used to investigate the frequency doubling (SHG) and to evaluate the crystal quality. The details of SHG measurements and results for m.NA-CNA crystals are given in reference 4. The quality of beam converting to green light is shown in Figure 7. Figure 7(a) shows significant scattering around the central beam. This scattering of light is due to inhomogeneity in the refractive indices of the m.NA-CNA crystal. The beam

conversion with better optical quality crystal is shown in Figure 7(b). This shows a more concentrated beam of light with less scattering due to better optical homogeneity. This type of test for m.NA-p.NA crystal is still in progress.

## 4. SUMMARY

Single crystals of doped m.nitroaniline were grown by a modified Bridgman growth method. Silicone oil and ethylene glycon were used to achieve the desired high thermal gradient without raising the temperature of the hot zone above the decomposition temperature of nitroanilines. The combination of source material purification and of a thermal gradient of 18 K/cm produced good quality m.NA-CNA and m.NA-p.NA crystals. Binary crystals showed less cleaving tendency compared to pure m.NA crystals. The crystal of m.NA-p.NA showed absorption bands between 0.5 and 0.85 micrometer wavelength region due to residual impurities.

## ACKNOWLEDGEMENTS

We are thankful to the Materials Directorate, Wright Laboratory, Wright-Patterson, AFB, Ohio, for the financial support under contract No. F33615-88-C-5506. We thank NASA, George Marshall Space Center for the partial support to prepare the cartridges of m.NA-p.NA system through purchase order H-20124, DCN 2-3-10-34841.

## 5. REFERENCES

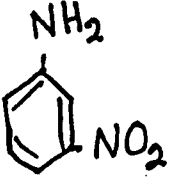

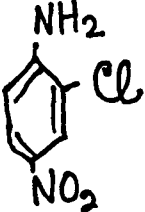
1. N. B. Singh and M. E. Glicksman, *J. Crystal Growth* 98 (1989) 534.
2. N. B. Singh, R. H. Hopkins, R. Mazelsky, N. Singh, and D. Lemmon, *J. Crystal Growth* 106 (1990) 106.
3. N. B. Singh, R. H. Hopkins, R. Mazelsky, R. N. Singh, N. Singh, and O. P. Singh, *Thermo. Chim. Acta* 159 (1990) 297.
4. N. B. Singh, T. Henningsen, R. H. Hopkins, R. Mazelsky, R. D. Hamacher, E. P. Supertzi, F. K. Hopkins, D. E. Zelmon, and O. P. Singh, *J. Crystal Growth* 128 (1993) 976.
5. R. P. Rastogi, N. B. Singh, and N. B. Singh, *J. Crystal Growth* 37 (1977) 329.

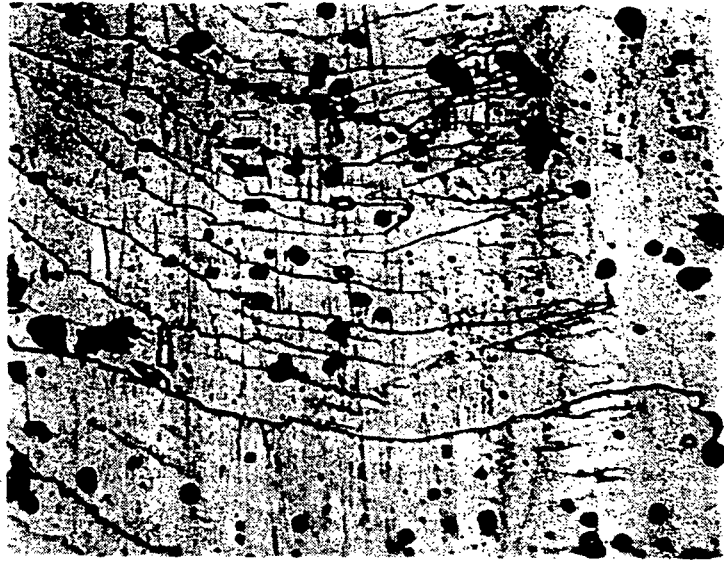
## CAPTIONS FOR FIGURES

- Figure 1 (a) m.NA-CNA crystal with impurity particles embodied in the bulk,  
(b) m.NA-CNA crystal with relatively few impurity particles in the bulk.
- Figure 2 Temperature distribution of the furnace (a) without and (b) with the heat transfer liquids. (Circle, triangle, and square denotes different sets of measurements.)
- Figure 3 Partial phase-diagram for m.NA-p.NA system.
- Figure 4 Bulk transparency of m.NA-p.NA crystal (a) with and (b) without wire mesh.
- Figure 5 Bulk transparency of m.NA-CNA crystal (a) with and (b) without wire mesh.
- Figure 6 Transmission curves for (a) m.NA-p.NA and (b) m.NA-CNA crystals.
- Figure 7 SHG experiment through a (a) crystal which shows large scattering and  
(b) crystal with good optical quality.

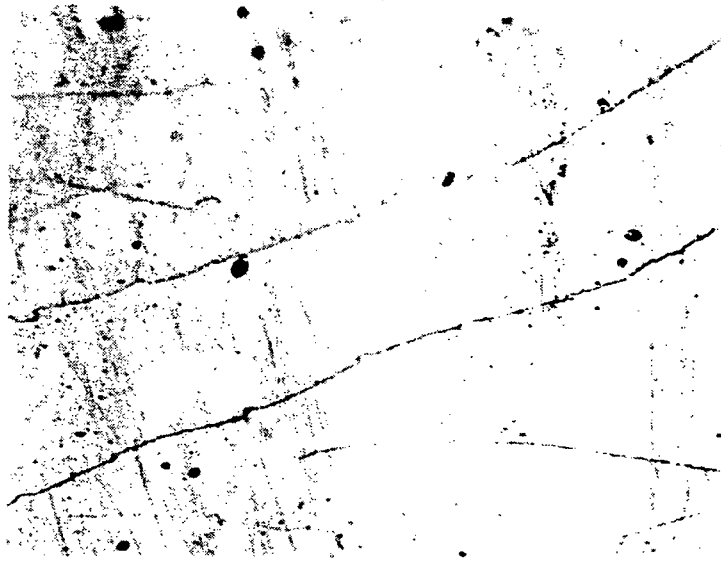
Table 1

## Properties of m.NA, p.NA and CNA

Properties	m.NA	p.NA	CNA
Chemical formula			
Heat of fusion (cal/g)	41.6	36.4	25.5
Crystal system	Orthorhombic biaxial	Monoclinic --	Orthorhombic biaxial
Lattice parameter (Å)	a = 6.485 b = 19.306 c = 5.087 Z = 4	a = 12.347 b = 5.997 c = 8.583 Z = 4	a = 4.109 b = 13.515 c = 14.183 Z = 4

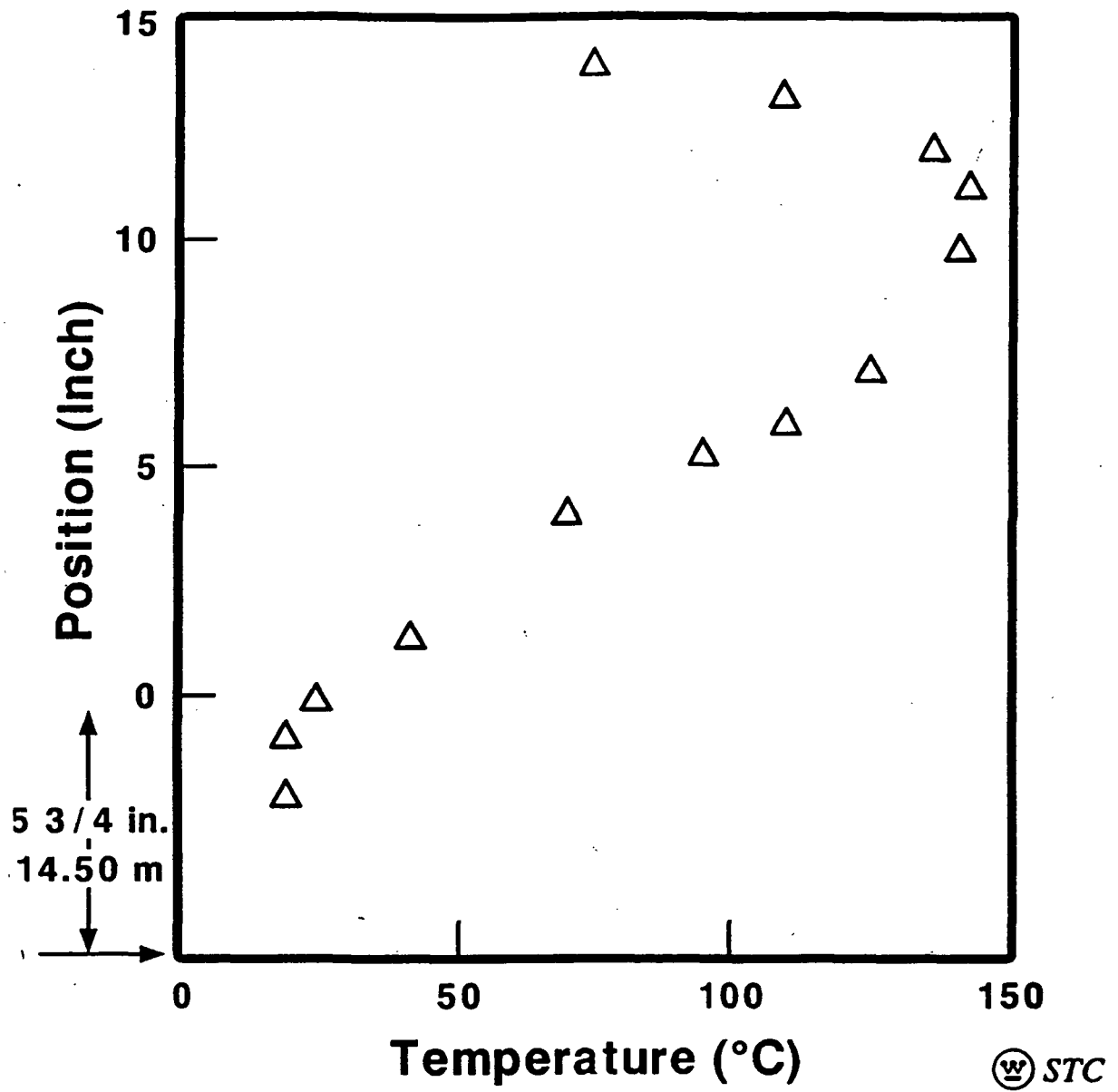


(a)



(b)

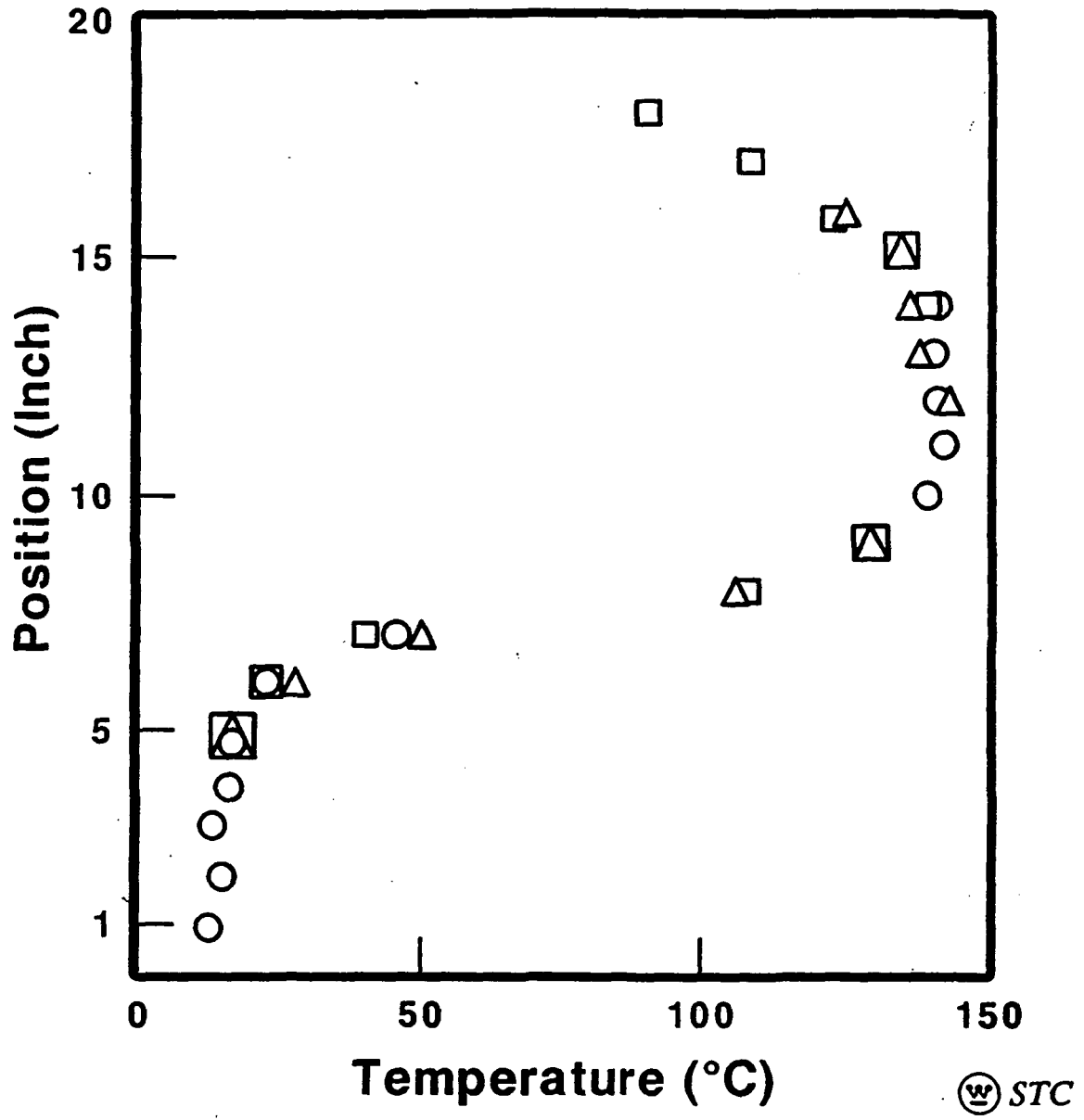
Fig.1



(a)

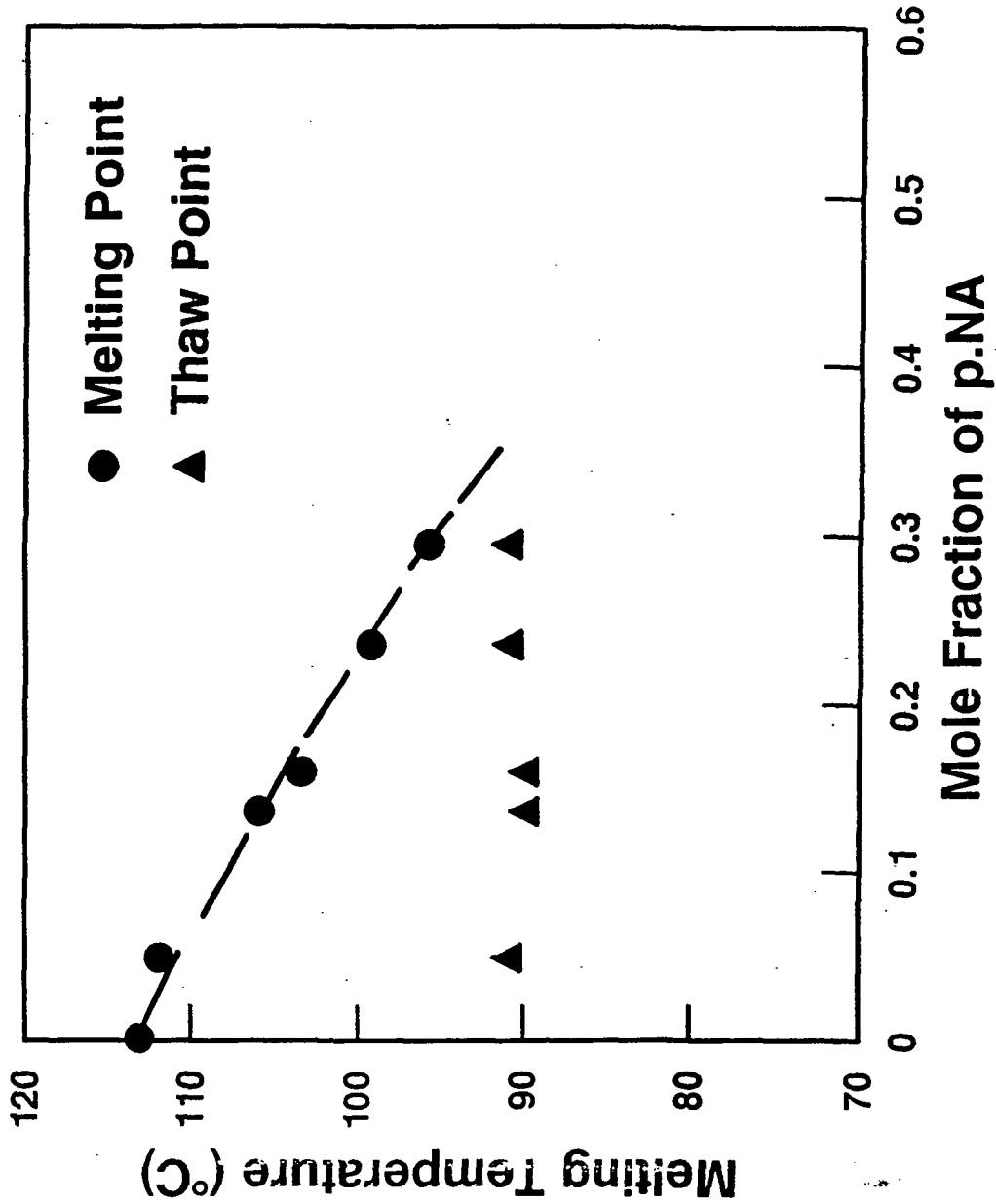
Fig. 2





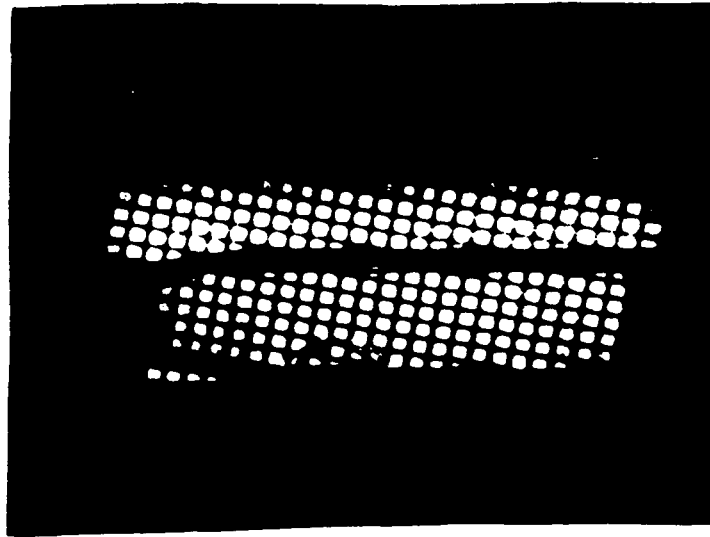
(b)

# PARTIAL PHASE-DIAGRAM FOR m.NA - p.NA SYSTEM

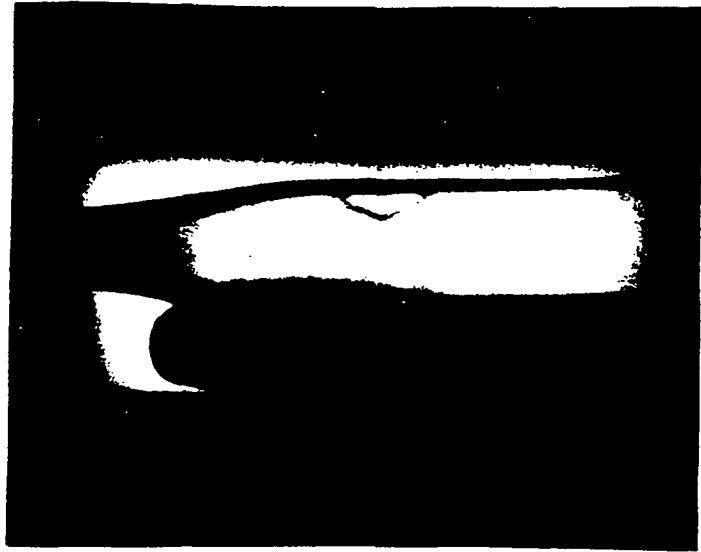


Ⓢ STC

Fig. 3

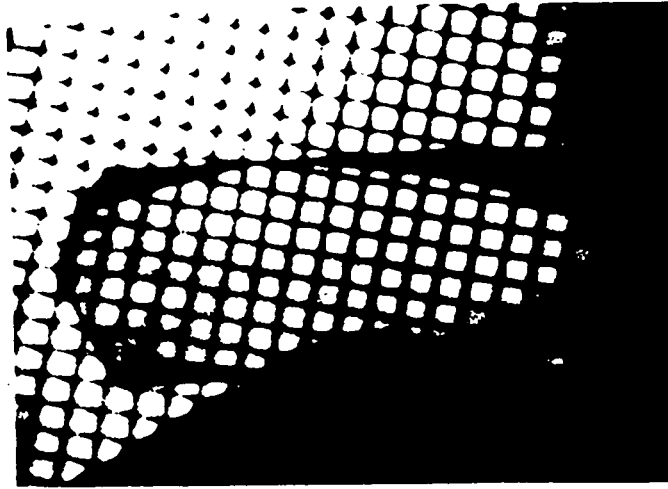


(a)

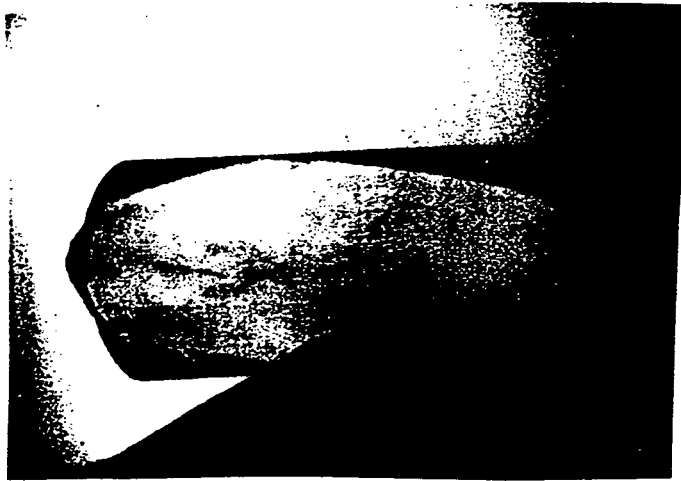


(b)

**Fig. 4**



(a)



(b)

**Fig. 5**

Curve 783665-A

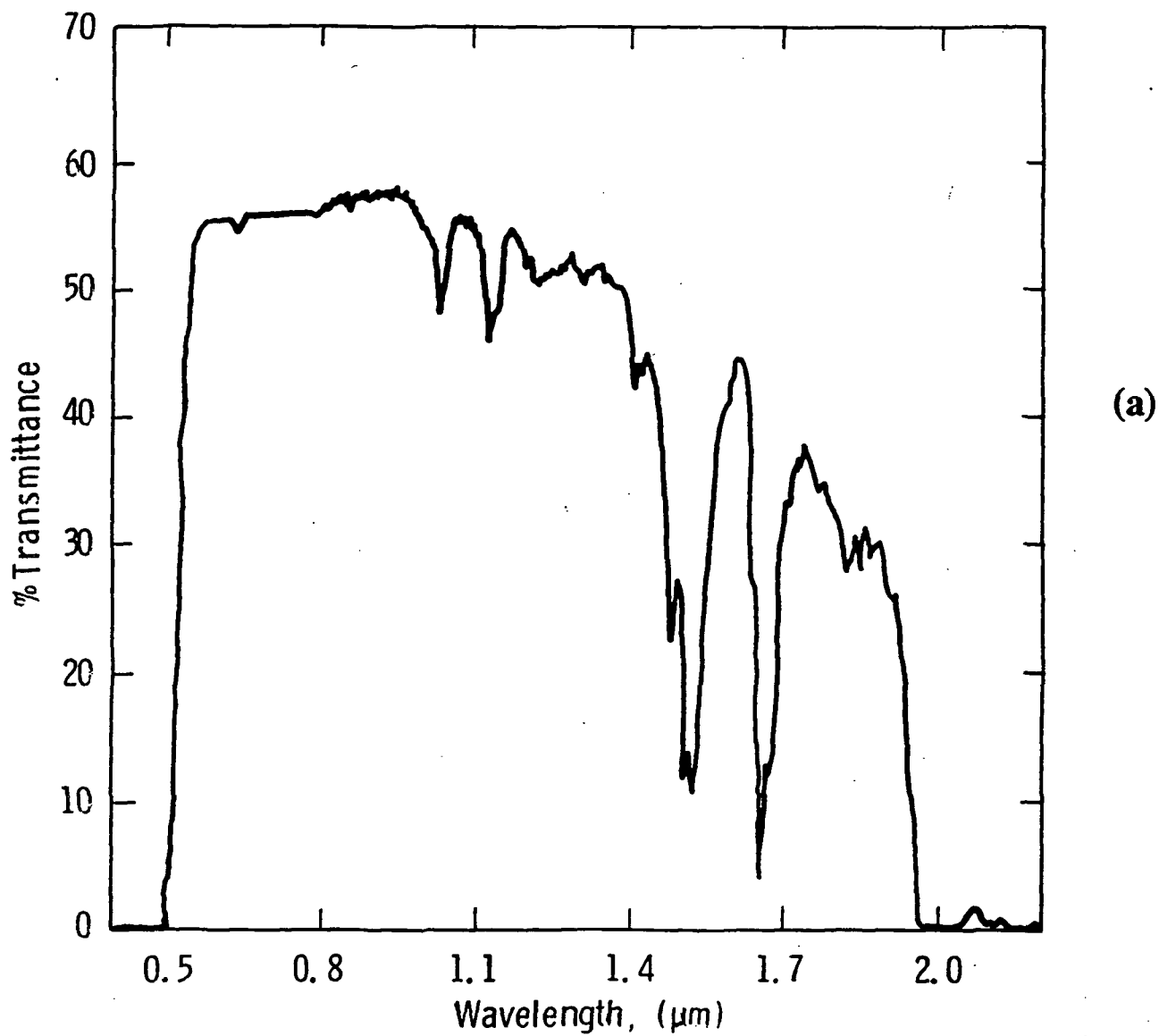
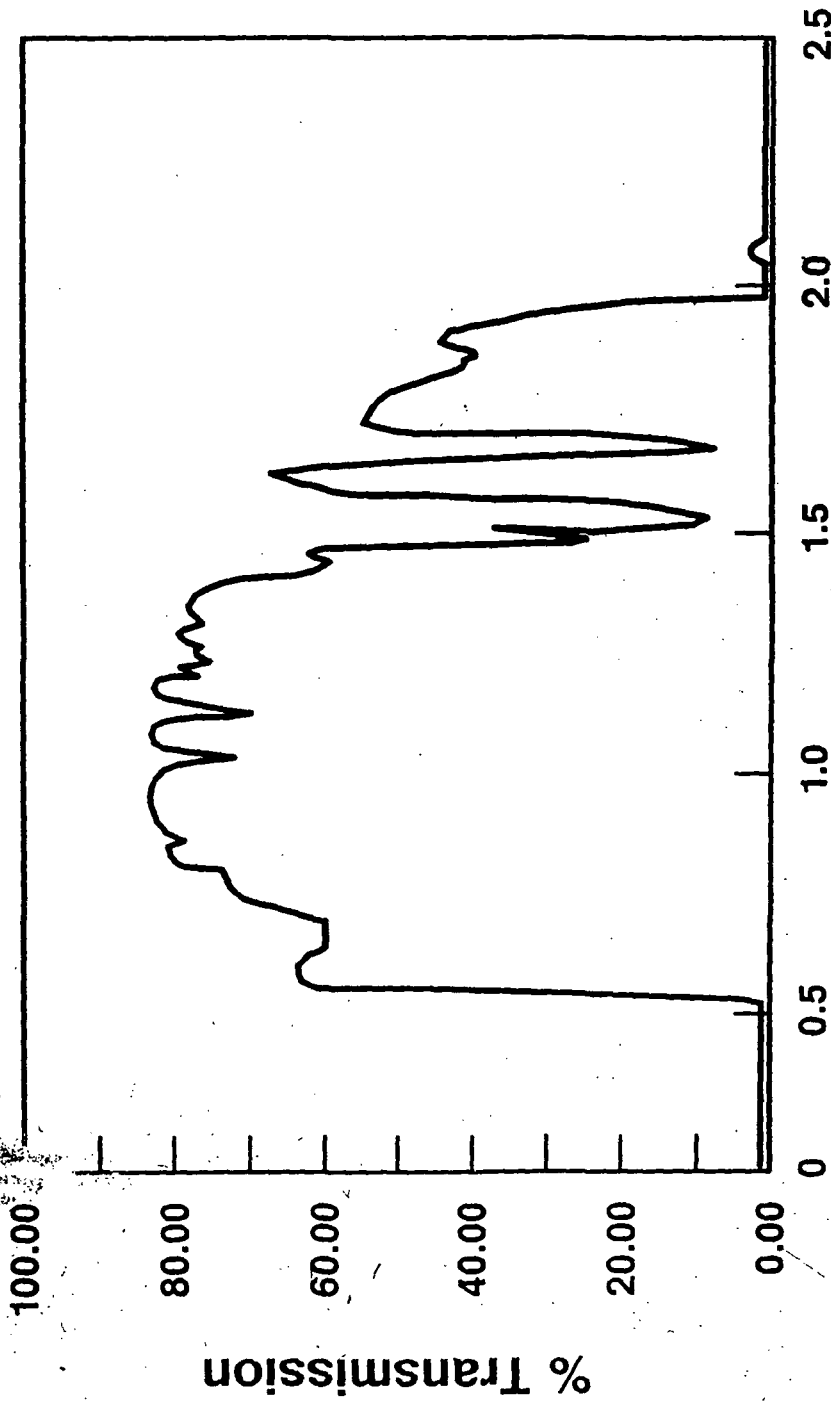


Fig. 6



STC

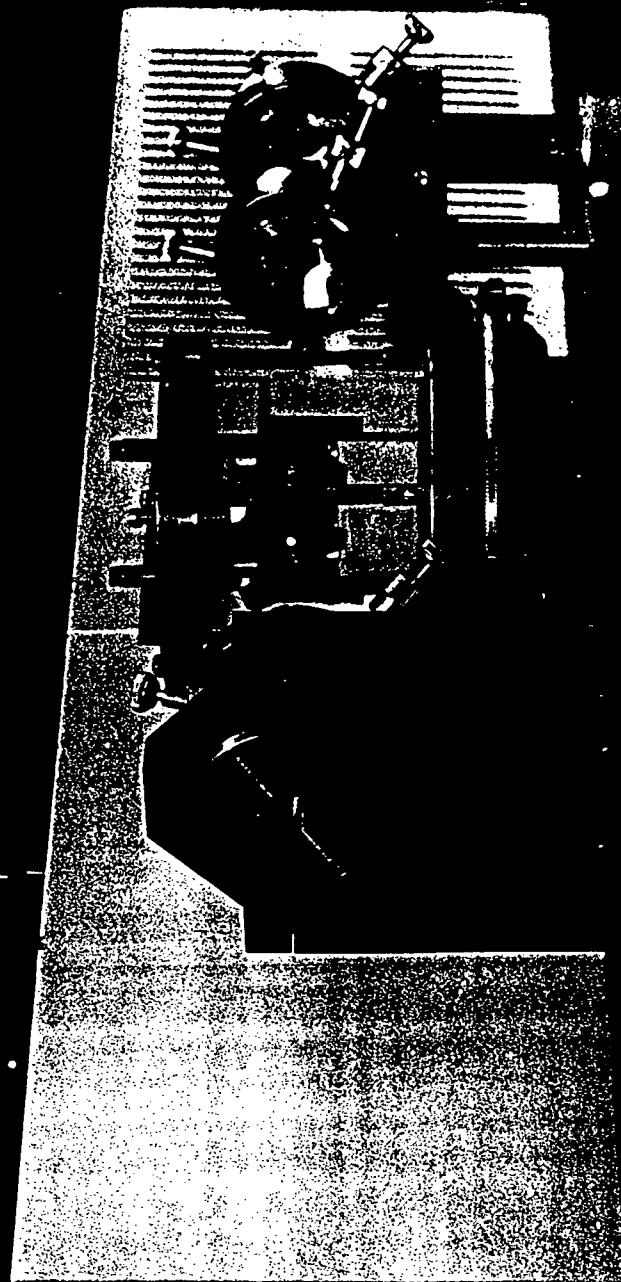
Fig. 6

ORIGINAL PAGE IS  
OF POOR QUALITY

(a)

Fig. 7

ORIGINAL PAGE IS  
OF POOR QUALITY



(b)

Fig. 7

ORIGINAL PAGE IS  
OF POOR QUALITY